Catalysis Today 151 (2010) 29–33

Contents lists available at ScienceDirect

Catalysis Today

journal homepage: www.elsevier.com/locate/cattod

UV-A/TiO_2 photocatalytic decomposition of erythromycin in water: Factors affecting mineralization and antibiotic activity

Nikolaos P. Xekoukoulotakis [a,*], Nikolaos Xinidis [a], Maria Chroni [a], Dionissios Mantzavinos [a], Danae Venieri [a], Evroula Hapeshi [b], Despo Fatta-Kassinos [b]

[a] Department of Environmental Engineering, Technical University of Crete, Polytechneioupolis, GR-73100 Chania, Greece
[b] Department of Civil and Environmental Engineering, University of Cyprus, 75 Kallipoleos St., 1678 Nicosia, Cyprus

ARTICLE INFO

Article history:
Available online 18 February 2010

Keywords:
Erythomycin
Mineralization
Antibiotic acivity
Photocatalysis
TiO_2
Water

ABSTRACT

The photocatalytic mineralization of the antibiotic erythromycin (ERM) in aqueous TiO_2 suspensions was investigated. UV-A irradiation was provided by a 9 W lamp at a photon flux of 4.69×10^{-6} einstein/s and runs were performed at ERM initial concentrations between 2.5 and 30 mg/L, 10 commercially available TiO_2 catalysts at loadings between 100 and 750 mg/L and at acidic or near neutral conditions. The extent to which the aforementioned factors influence ERM mineralization was assessed measuring the total organic carbon (TOC) content of the solution. Of the various catalysts tested, Degussa P25 (75:25, anatase:rutile) was highly active yielding 90% TOC reduction after 90 min of reaction with 10 mg/L ERM and 250 mg/L TiO_2; the second best catalyst consisting of pure anatase (Hombikat UV 100) yielded only 65% reduction. TOC removal decreased with decreasing titania loading and increasing ERM concentration and solution pH. For the range of the ERM concentrations studied, mineralization kinetics appears to follow the Langmuir–Hinshelwood model. Short (i.e. 15 min) photocatalytic treatment of 30 mg/L ERM was capable of abolishing completely the antimicrobial properties of ERM to *E. coli* but this was accompanied by insignificant levels (i.e. 10%) of total oxidation.

1. Introduction

Over the past few years, pharmaceuticals are considered as an emerging environmental problem due to their continuous input and persistence into the aquatic ecosystem even at low concentrations. After their use, human pharmaceuticals or their metabolites are excreted into the effluents and reach the sewage treatment plants (STPs). Unfortunately, conventional STPs are not able to degrade residues of pharmaceutical compounds, and as a result they are introduced into the aquatic environment. Residual amounts of pharmaceuticals can reach surface waters, groundwater or sediments. Many studies have reported a large number of pharmaceuticals at concentrations ranging from ng/L to μg/L in STP effluents, in natural waters and even in drinking water [1–3].

The concern regarding the presence of pharmaceuticals in STP effluents and natural waters has provoked the development of methods capable of removing pharmaceutical residues efficiently. Based on this need, various advanced oxidation processes have been investigated, due to their potential as alternatives or as a complement to conventional wastewater treatment. These processes are characterized by the formation of hydroxyl radicals, which exhibit high reactivity and efficiency in oxidizing a great variety of organic micropollutants, including pharmaceuticals [4].

Among the various pharmaceutical compounds present in the environment, special emphasis has been given to antibiotics, which are the most often discussed pharmaceuticals because of their potential role in the development of antibiotic-resistant bacteria [1,5]. Antibiotics are used extensively in human and veterinary medicine, as well as in aquaculture, for the purpose of preventing or treating microbial infections [6]. They are often partially metabolized in the organism and they are excreted as the parent substance or as metabolites into wastewaters. Most antibiotics tested to date are not biodegradable under aerobic conditions [6].

Erythromycin (ERM) is a glycosidic 14-membered ring macrolide, which is widely used as an antibacterial antibiotic and produced by the Gram-positive filamentous bacterium *Saccharopolyspora erythraea* [7]. ERM has been found in concentrations ranging from ng/L to μg/L in STP effluents, surface waters and groundwater [6,8]. There have been few studies on the oxidative degradation of ERM in wastewaters reporting the use of ozonation alone [9–12], ozone in combination with H_2O_2 (11) or UV (12), UV

* Corresponding author at: Department of Environmental Engineering, Technical University of Crete, University Campus, Polytechneioupolis, GR-73100 Chania, Crete, Greece. Tel.: +30 2821037796; fax: +30 2821035852.
E-mail address: nikos.xekoukoulotaki@enveng.tuc.gr (N.P. Xekoukoulotakis).

0920-5861/$ – see front matter © 2010 Elsevier B.V. All rights reserved.
doi:10.1016/j.cattod.2010.01.040

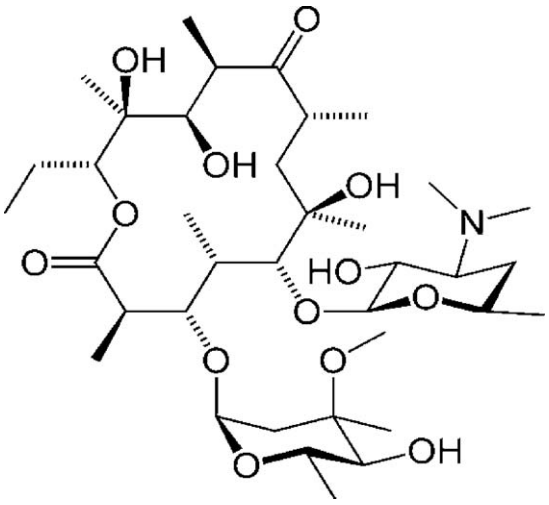

Scheme 1. The molecular structure of erythromycin.

in combination with H_2O_2 (12), oxidation with free chlorine and monochloramine [13] and a combination of anodic oxidation by boron-doped diamond electrodes and ozonation [14].

The aim of the present work was to study the photocatalytic oxidation of ERM in aqueous solutions using TiO_2 as a catalyst under UV-A irradiation; to the best of our knowledge, this has not yet been reported in the literature. We investigated in a systematic way the effect of various operating conditions such as TiO_2 type and loading, ERM initial concentration and solution pH on mineralization in model aqueous solutions. Moreover, the effect of photocatalytic treatment on the antimicrobial properties of ERM was assessed. We intentionally decided to investigate sample mineralization rather than substrate decomposition since the rationale of micro-pollution abatement in aqueous matrices should involve its complete elimination rather than its transformation to other species.

2. Materials and methods

2.1. ERM and catalysts

ERM ($C_{37}H_{67}NO_{13}$ shown in Scheme 1) of 95% purity was purchased from Fluka and used as received. Model solutions of ERM were prepared in ultrapure water (resistivity 18.2 MΩ cm at 25 °C) prepared on a water purification system (EASYpureRF) supplied by Barnstead/Thermolyne (USA). Ten commercially available TiO_2 samples, whose main properties as given by the manufacturers are summarized in Table 1, were employed in this study for slurry photocatalytic experiments.

2.2. Photocatalytic experiments

UV-A irradiation was provided by a 9 W lamp (Radium Ralutec, 9W/78) emitting predominantly at 350–400 nm. The photon flux emitted from the lamp was determined actinometrically using the potassium ferrioxalate method and was found to be 4.69×10^{-6} einstein/s. Experiments were conducted in an immersion well, batch type, laboratory scale photoreactor, purchased from Ace Glass (Vineland, NJ, USA) and described in detail elsewhere [15].

In a typical photocatalytic run, 350 mL of the aqueous solution containing the desired concentration of ERM in the range 2.5–30 mg/L (these values are well below ERM solubility in water which has been reported to be 2–2.1 g/L [7,16]) were loaded in the reaction vessel. These concentrations, although considerably greater than those typically found in environmental samples, were chosen to allow (i) the assessment of process efficiency within a measurable time scale and (ii) the accurate determination of residual organic carbon with the analytical techniques employed in this work. The solution was slurried with the appropriate amount of catalyst and magnetically stirred for 30 min in the dark to ensure complete equilibration of adsorption/desorption of ERM onto the TiO_2 surface. After that period, the UV-A lamp was turned on, while pure O_2 was continuously sparged (unless otherwise stated) in the liquid under stirring. During photocatalytic experiments, temperature was maintained at 25 °C with a temperature control unit. In most cases, experiments were performed at ambient solution pH which was acidic in the order 4–5.7 (depending on ERM initial concentration and type of catalyst) and left uncontrolled during the reaction. For those runs carried out at near neutral conditions, the initial pH was adjusted adding the appropriate amount of 2N NaOH solution. In all cases, it was found that the pH of the solution was practically constant during the course of the reaction. Photocatalytic experiments were performed in duplicate and mean values are quoted as results.

2.3. Mineralization

Samples periodically taken from the reactor were centrifuged at 13,100 rpm to remove catalyst particles and then analyzed for their total organic carbon (TOC) content on a Shimadzu 5050A TOC analyzer, whose operation is based on the catalytic combustion/non-dispersive infrared gas analysis, to assess the extent of total oxidation that had occurred. TOC analysis was run in triplicate with relative standard deviation never exceeding 10% in the range of concentrations studied.

2.4. Antibiotic susceptibility assay

Antibiotic susceptibility was determined by the agar diffusion method (Bauer–Kirby) [17] in accordance with NCCLS guidelines M23-A2 and M37-A2 [18,19], using *Escherichia coli* ATCC 23716 as

Table 1
TiO_2 catalysts used in this study.

Catalyst	Crystal form	BET area (m^2/g)	Particle size (nm)	Supplier
Degussa P25	75%A:25%R	50	21	Degussa AG
Hombikat UV 100	A > 99%	<250	5	Sachleben Chemie GmbH
Millennium PC 50	A > 97%	45–55	20–30	Millennium Inorganic Chemicals
Millennium PC 100	A > 95%	80–100	15–25	Millennium Inorganic Chemicals
Millennium PC 105	A > 95%	75–95	15–25	Millennium Inorganic Chemicals
Millennium PC 500	A > 75%	<300	5–10	Millennium Inorganic Chemicals
Aldrich	A > 99%	190–290	15	Aldrich
Tronox A-K-1	A > 97%	90	20	Kerr-McGee Chemicals LLC
Tronox TR-HP-2	99.7%R	7	ND	Kerr-McGee Chemicals LLC
Tronox TR	99.5%R	5.5	300	Kerr-McGee Chemicals LLC

A, anatase; R, rutile; ND, not determined.

reference strain. Following photocatalytic oxidation, samples of 0.5 mL were pipetted onto 13 mm diameter antibiotic disks (Whatman) which were dried at 35 °C for 60 min. The medium used for all tests was Mueller–Hinton agar (Merck). The entire surface of each Mueller–Hinton plate was inoculated by streaking with a sterile cotton swab containing the inoculum of the reference strain. The disks containing the test substrates were applied on plates, which were incubated at 35 °C for 24 h. A calibration curve was also prepared performing controls with ERM at different concentrations in the range of 10–60 mg/L.

3. Results and discussion

3.1. Preliminary screening experiments

To assess the relative catalytic activity of various TiO_2 samples, preliminary experiments were conducted at 10 mg/L ERM initial concentration, 250 mg/L catalyst loading and ambient solution pH of about 4.7. Fig. 1 shows that almost 90% TOC reduction could be achieved after 90 and 150 min of reaction with Degussa P25 and Hombikat UV 100 catalysts, respectively, while all other TiO_2 samples yielded <75% mineralization after 150 min. Tronox TR-HP-2 gave practically no mineralization and, therefore, respective data are not included in Fig. 1. To confirm the beneficial role of photocatalysis on ERM mineralization, an additional experiment was performed in the absence of catalyst; in this case, photolytic mineralization remained as low as 5% after 120 min of irradiation. There have been several papers explaining why Degussa P25 exhibits higher photocatalytic activity than other TiO_2 photocatalysts. Some authors [20,21] attribute this to the slower electron/hole recombination taking place on the surface of Degussa P25 compared to other TiO_2 photocatalysts like Hombikat UV100. Other authors [22] ascribe the higher activity of Degussa P25 to its structure which is a mixture of anatase and rutile; this mixture is more active than the individual pure crystalline phases. According to the above findings, all subsequent photocatalytic experiments were performed with Degussa P25 TiO_2.

To verify the positive role of electron acceptors in the photocatalytic process, an additional experiment was performed without oxygen sparging and the results are shown in Fig. 2. Oxidation for 90 min of 10 mg/L ERM with 500 mg/L Degussa P25 at ambient pH of 4.6 and continuous aeration led to complete mineralization, while the respective value without aeration was only 35%. This is due to oxygen trapping of the photogenerated conduction band electrons to form superoxide radical anions as follows:

$$e_{CB}^- + O_2 \rightarrow O_2^{\bullet -} \quad (1)$$

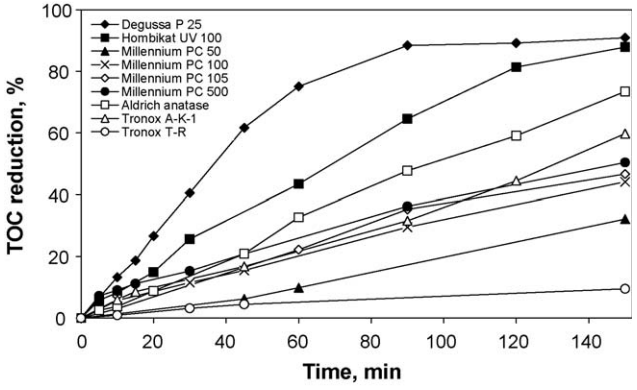

Fig. 1. Relative activity of various TiO_2 samples (250 mg/L) for 10 mg/L ERM mineralization.

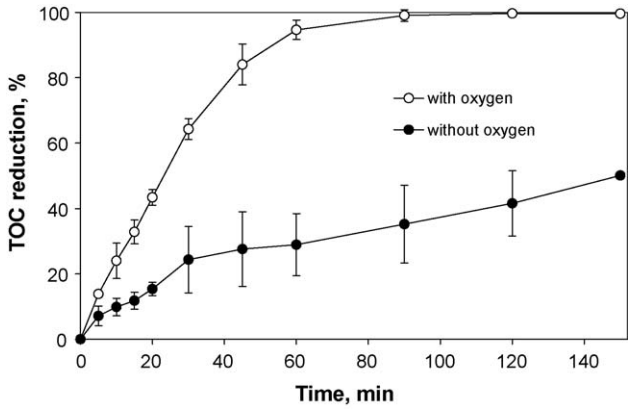

Fig. 2. Effect of oxygen sparging on 10 mg/L ERM mineralization with 500 mg/L Degussa P25. Error bars show standard deviation of duplicate runs.

Reaction (1) is critical to the photocatalytic performance for two reasons, namely: (i) the undesirable recombination of electrons and valence band holes is minimized and (ii) more reactive oxygen species are formed since superoxide radical anions may react with protons formed through water splitting to yield peroxide radicals as follows:

$$O_2^{\bullet -} + H^+ \rightarrow HO_2^{\bullet} \quad (2)$$

3.2. Effect of catalyst loading

TiO_2 loading in slurry photocatalytic processes is an important factor that can influence strongly the mineralization of the organic pollutant. The effect of Degussa P25 loading on 10 mg/L ERM mineralization was studied in the range 100–750 mg/L and ambient solution pH of about 5 and the results are shown in Fig. 3. As seen, mineralization increased with increasing catalyst concentration up to about 500 mg/L after which it remained practically unchanged. The increase in photocatalytic activity with increasing catalyst loading indicates a heterogeneous catalytic regime since the fraction of incident light absorbed by the semiconductor progressively increases in suspensions containing higher amounts of TiO_2. However, photocatalytic activity reached a plateau at about 500 mg/L TiO_2 loading. The catalyst concentration above which conversion levels off depends on several factors (e.g. reactor geometry, operating conditions, wavelength and intensity of light source) and corresponds to the point where all catalyst particles, i.e. all the surface exposed, are fully illuminated [23]. At higher concentrations, a screening effect of excess particles occurs,

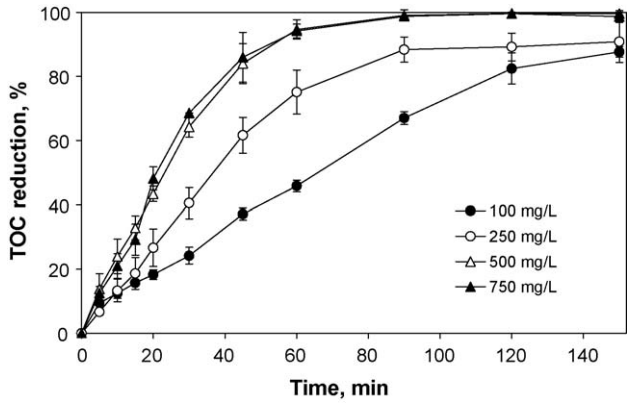

Fig. 3. Effect of Degussa P25 loading on 10 mg/L ERM mineralization. Error bars show standard deviation of duplicate runs.

thus masking part of the photosensitive surface and consequently hindering light penetration; this usually results in conversion reaching a plateau, while at excessive catalyst concentrations conversion may also decrease due to increased light reflectance onto the catalyst surface. In this study, the optimum concentration at which all subsequent experiments were conducted was about 500 mg/L.

3.3. Effect of ERM concentration

The effect of varying ERM initial concentration was studied in the range 2.5–30 mg/L at 500 mg/L Degussa P25 loading and the results are shown in Fig. 4a. As seen, conversion expectedly increased with decreasing concentration, e.g. after 30 min its value was 77, 65 and 19% at 2.5, 5 and 30 mg/L ERM, respectively. From an engineering point of view though, what is important is the amount of pollutant destroyed rather than the conversion itself. In this perspective, performance increased with increasing concentration since after, e.g. 30 min of reaction the amount of organic carbon mineralized was about 1.1, 1.7 and 2.6 mg/L, respectively.

Photocatalytic degradation usually follows the Langmuir–Hinshelwood model [23] which in terms of mineralization kinetics can be described as follows:

$$r_0 = -\frac{d\mathrm{TOC}}{dt} = k_r\theta = k_r\frac{K\mathrm{TOC_{eq}}}{1+K\mathrm{TOC_{eq}}} \Leftrightarrow \frac{\mathrm{TOC_{eq}}}{r_0} = \frac{1}{k_rK} + \frac{\mathrm{TOC_{eq}}}{k_r} \quad (3)$$

where r_0 is the initial rate of mineralization (mg/(L min)), t is the illumination time (min), k_r is the reaction rate constant (mg/(L min)), θ is the coverage of the catalyst surface, K is the equilibrium constant for adsorption of the organics onto TiO_2 surface (L/mg) and $\mathrm{TOC_{eq}}$ is the equilibrium concentration of the organic carbon (mg/L). The ratio $\mathrm{TOC_{eq}}/r_0$ was calculated for the various initial ERM concentrations and plotted against $\mathrm{TOC_{eq}}$; as can be seen in Fig. 4b, a straight line fitted the experimental data

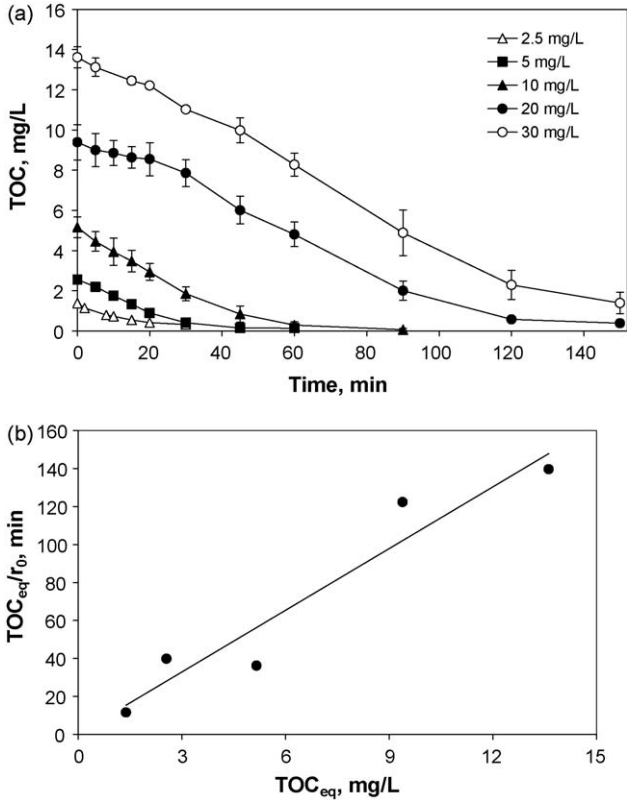

Fig. 4. (a) Effect of initial ERM concentration on mineralization with 500 mg/L Degussa P25. Error bars show standard deviation of duplicate runs and (b) plot of Eq. (3).

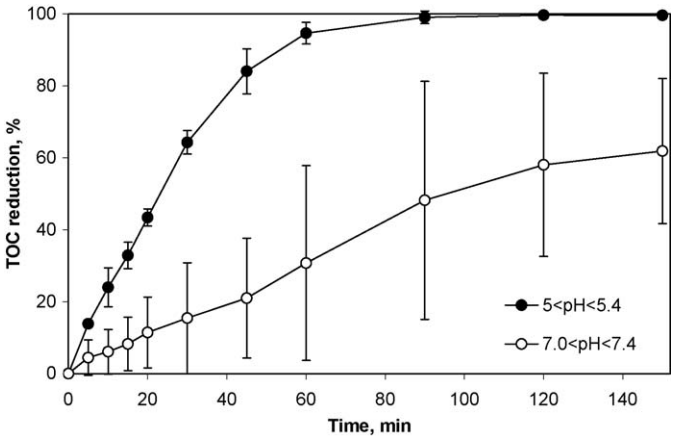

Fig. 5. Effect of initial solution pH on 10 mg/L ERM mineralization with 500 mg/L Degussa P25. Error bars show standard deviation of duplicate runs.

reasonably well (the coefficient of linear regression, r, was 0.96), thus indicating that photocatalytic mineralization of ERM most probably follows Langmuir–Hinshelwood kinetics. From the slope of the straight line, k_r was computed equal to 0.092 mg/(L min), while from the intercept, K was 26.2 L/mg.

3.4. Effect of initial solution pH

Fig. 5 shows the effect of initial solution pH on 10 mg/L ERM mineralization at 500 mg/L Degussa P25. Mineralization was favored at solution's natural pH of 5.2 ± 0.2, while near neutral conditions (7.2 ± 0.2) impeded degradation. The effect of pH on degradation is a complex issue since it governs (i) the equilibrium of water dissociation which, in turn, affects the level of hydroxyl radicals generation, (ii) the surface charge of titania with respect to its point of zero charge (pzc), (iii) the ionization state of ERM (whose pK_a is 8.8 [7,16]) and its degradation products, and (iv) the oxidative power of the photogenerated holes [24]. At pH < 6.7 which is the pzc of Degussa P25 [25] the surface becomes positively charged, while at pH > 6.7 it becomes negatively charged. Given that the action of photogenerated holes is favored at acidic conditions, while hydroxyl radicals become the dominant species at neutral and alkaline conditions, this could explain the fast ERM mineralization at lower pH values. Furthermore and on the assumption that ERM degradation products are mostly negatively charged, this would also explain the discrepancy between acidic and neutral conditions since the former would favor the electrostatic attraction between organics and the catalyst surface.

3.5. Antibiotic activity

Fig. 6a shows the correlation between the antibiotic activity of ERM and its concentration in the range 10–60 mg/L. At concentrations up to 10 mg/L, ERM exhibited no such activity to *E. coli* since an inhibition zone of 13 mm was recorded corresponding to the diameter of the testing plate (shown by the dotted line); above this concentration, there appears to be a linear relationship between concentration and activity (the coefficient of linear regression, r, was 0.99). Fig. 6b shows the effect of photocatalytic oxidation at 500 mg/L Degussa P25 on the antimicrobial properties of 30 mg/L ERM. Short treatment for 5 min led to partial removal of the antibiotic activity of ERM to *E. coli* with the residual ERM concentration being about 20 mg/L (according to Fig. 6a); treatment for another 5–10 min eliminated completely the activity, thus corresponding to a residual ERM concentration of not more than 10 mg/L. At these conditions, only about 10% mineralization occurred (according to Fig. 4a), thus implying that ERM degradation intermediates possess no antibiotic activity.

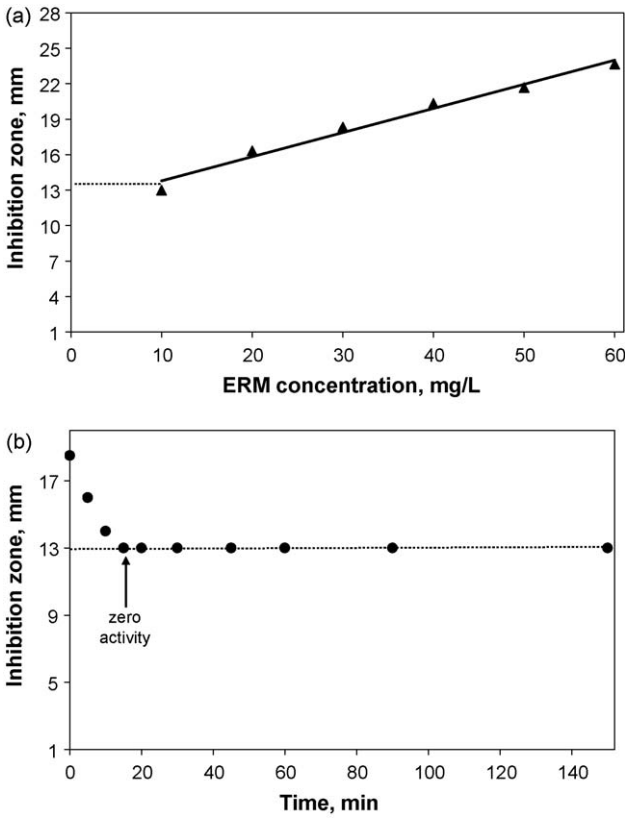

Fig. 6. (a) Correlation between antibiotic activity and ERM concentration and (b) change of antibiotic activity of 30 mg/L ERM during photocatalytic oxidation with 500 mg/L Degussa P25.

4. Conclusions

The conclusions drawn from the present study can be summarized as follows:

(1) Semiconductor photocatalysis based on Degussa P25 TiO_2 is an efficient method for the mineralization of erythromycin in aqueous solutions. Process performance is affected by several factors, namely irradiation time, photocatalyst type and loading, the presence of electron acceptors and solution pH.
(2) Mineralization (in terms of carbon conversion to CO_2) is enhanced at lower concentrations. Since the levels of erythromycin and alike compounds in environmental samples are relatively low (e.g. 2–3 orders of magnitude lower than those employed in this work), their degradation is likely to occur readily at mild operating conditions.
(3) Degradation intermediates do not have antimicrobial properties against *E. coli* as assessed by the agar diffusion assay.

Acknowledgement

The authors are grateful to the Cyprus Research Promotion Foundation for funding this research project (PHAREM-AEIFO/0506/16).

References

[1] T.A. Ternes, A. Joss, Human Pharmaceuticals, Hormones and Fragrances: The Challenge of Micropollutants in Urban Water Management, first ed., IWA, Cornwall, 2006.
[2] K. Kümmerer, Pharmaceuticals in the Environment: Sources, Fate, Effects and Risks, third ed., Springer, Berlin, 2008.
[3] A. Nikolaou, S. Meric, D. Fatta, Anal. Bioanal. Chem. 387 (2007) 1225–1234.
[4] M. Klavarioti, D. Mantzavinos, D. Kassinos, Environ. Int. 35 (2009) 402–417.
[5] K. Kümmerer, Chemosphere 75 (2009) 435–441.
[6] K. Kümmerer, Chemosphere 75 (2009) 417–434.
[7] S. Omura, Macrolide Antibiotics: Chemistry, Biology and Practice, second ed., Academic Press, San Diego, 2002.
[8] I. Munoz, M.J. Gomez-Ramos, A. Aguera, J.F. Garcia-Reyes, A. Molina-Diaz, A.R. Fernandez-Alba, Trends Anal. Chem. 28 (2009) 676–694.
[9] T.A. Ternes, J. Stüber, N. Herrmann, D. McDowell, A. Ried, M. Kampmann, B. Teiser, Water Res. 37 (2003) 1976–1982.
[10] N Nakada, H. Shinohara, A. Murata, K. Kiri, S. Managaki, N. Sato, H. Takada, Water Res. 41 (2007) 4373–4382.
[11] A.Y.-C. Lin, C.-F. Lin, J.-M. Chiou, P.K.A. Hong, J. Hazard. Mater. 171 (2009) 452–458.
[12] I.K. Kim, N. Yamashita, Y. Kato, H. Tanaka, Water Sci. Technol. 59 (2009) 945–955.
[13] E. Chamberlain, C. Adams, Water Res. 40 (2006) 2517–2526.
[14] H.M Menapace, N. Diaz, S. Weiss, J. Environ. Sci. Health A 43 (2008) 961–968.
[15] C. Fotiadis, N.P. Xekoukoulotakis, D. Mantzavinos, Catal. Today 124 (2007) 247–253.
[16] A.T. Florence, D. Attwood, Physicochemical Principles of Pharmacy, fourth ed., Pharmaceutical Press, London, 2006.
[17] A.W. Bauer, W.M. Kirby, J.C. Sherris, M. Turck, Tech. Bull. Regist. Med. Technol. 36 (1966) 49–52.
[18] National Committee for Clinical Laboratory Standards, Development of In Vitro Susceptibility Testing Criteria and Quality Control Parameters. Approved Guideline M23-A2, National Committee for Clinical Laboratory Standards, Wayne, PA, 2001.
[19] National Committee for Clinical Laboratory Standards, Performance Standards for Antimicrobial Disk and Dilution Susceptibility Tests for Bacteria Isolated from Animals. Approved Standard M31-A2, National Committee for Clinical Laboratory Standards, Wayne, PA, 2002.
[20] S.T. Martin, H. Herrmann, W. Choi, M.R. Hoffmann, J. Chem. Soc., Faraday Trans. 21 (1994) 3315–3322.
[21] C.A. Emilio, M.I. Litter, K. Marinus, M. Bouchard, C. Colbeau-Justin, Langmuir 22 (2006) 3606–3613.
[22] R.I. Bickley, T. Gonzalez-Carreno, J.S. Lees, L. Palmisano, R.J.D. Tilley, J. Solid State Chem. 92 (1991) 178–190.
[23] J.M. Hermann, Catal. Today 53 (1999) 115–129.
[24] H. Lachheb, E. Puzenat, A. Houas, M. Ksibi, E. Elaloui, C. Guillard, J.M. Hermann, Appl. Catal. B: Environ. 39 (2002) 75–90.
[25] P. Fernandez-Ibanez, J. Blanco, S. Malato, F.J. de las Nieves, Water Res. 37 (2003) 3180–3188.